



Hyperintense areas in the intraorbital optic nerve evaluated by T2-weighted magnetic resonance imaging: a glymphatic pathway?

Satoshi Tsutsumi¹ · Hideo Ono² · Hisato Ishii¹

Received: 3 October 2020 / Accepted: 4 December 2020 / Published online: 5 January 2021
© Springer-Verlag France SAS, part of Springer Nature 2021

Abstract

Purpose The present study aimed to explore the glymphatic pathway in the intraorbital optic nerve (ON) using magnetic resonance imaging (MRI).

Methods Following conventional MRI examination, a total of 89 outpatients underwent T2-weighted imaging in thin-sliced coronal and sagittal sections. Moreover, three injected cadaver heads were dissected.

Results In the cadaver specimens, differences in appearance between the central and peripheral parts of the ON were not observed. On the axial T2-weighted MRI performed in the initial examination, the central part of the intraorbital ONs was delineated as a well-demarcated, linear hyperintense area in 19% of patients. On the thin-sliced serial coronal images, the hyperintense areas were identified on both sides in 91% of patients. They were delineated as continuous hyperintense areas in the ONs with an inconsistent appearance even in the same nerve. In 12.4% of patients, the areas were divided into the upper and lower parts by a horizontal septum, while others showed variable morphologies, lacking a septum. On thin-sliced sagittal images, hyperintense areas were identified in 46% of patients.

Conclusion Hyperintense areas in the intraorbital ON detected on T2-weighted sequences may involve a glymphatic pathway with perivascular spaces of the ON and central retinal artery. These may be collapsed and difficult to identify on surgical and cadaver specimens.

Keywords Optic nerve · Central retinal artery · Hyperintense area · Glymphatic pathway

Introduction

The glymphatic system is known to be a network of perivascular spaces that promotes movement of the cerebrospinal fluid (CSF) into the brain and clearance of metabolic waste [12]. It was initially reported by Iliff et al. [7]. The fluid transport system is supported by the water channel aquaporin-4 under circadian control [5]. The intracranial and intraorbital parts of the optic nerve (ON) are surrounded by subarachnoid spaces that contain a complex system of arachnoid trabeculae and septa. Moreover, the ON is exposed to both CSF and intraocular pressures, which converge at the

lamina cribrosa [9, 13]. Recent studies have suggested that a glymphatic system exists in the ON, optic chiasm, optic tract, and primary visual cortex, as well as perivascular spaces of the central retinal artery (CRA) coursing in the central part of the ON [8, 10, 14, 22, 25]. The presence of a glymphatic pathway in the ON was first proposed by Wostyn et al. [19–21, 23] followed by histological verification of an ON perivascular pathway. Furthermore, variable pathological conditions disturbing the glymphatic pathways in the ONs have been shown to lead to ON dysfunction with decreased ON diameter, height of the optic chiasm, and volume of the lateral geniculate nucleus [1, 3, 4, 6, 11, 17, 18, 21, 23, 27]. The glymphatic hypothesis of glaucoma was initially documented by Mathieu et al. based on the theory proposed by Wostyn et al. [11, 19]. However, to the best of our knowledge, there has been no study visualizing the glymphatic pathway in the optic pathway with neuroimaging [4, 17, 18, 26, 27]. On the other hand, Jacobsen et al. [8] supposed the presence of a glymphatic system in the human visual pathway, including the ON, optic chiasm, optic tract,

✉ Satoshi Tsutsumi
shotaro@juntendo-urayasu.jp

¹ Department of Neurological Surgery, Juntendo University Urayasu Hospital, 2-1-1 Tomioka, Urayasu, Chiba 279-0021, Japan

² Division of Radiological Technology, Medical Satellite Yaesu Clinic, Tokyo, Japan

and primary visual cortex based on the examination using intrathecally infused gadolinium-enhanced magnetic resonance imaging (MRI).

The present study aimed to explore the glymphatic pathway in intraorbital ONs by cadaver dissection and MRI.

Materials and methods

This retrospective study included a total of 89 outpatients who presented to our hospital between August 2011 and September 2013 with headache, dizziness, vertigo, tinnitus, hemisensory disturbance, scintillating scotoma, and focal seizures. The patient population comprised 45 men and 44 women with age ranging from 12 to 81 years (mean, 53.6 ± 15.8 years). No patients had a history of glaucoma, inflammatory orbital diseases, autoimmune diseases of the central nervous system, orbital or brain tumor, traumatic orbital or brain injury, hydrocephalus, or meningitis. These pathologies were excluded by detailed interview and initial, conventional MRI examination using axial T1-weighted, T2-weighted, T2-gradient echo, fluid-attenuated inversion recovery, and diffusion-weighted sequences. The following parameters were used for axial T2-weighted imaging: repetition time, 3500.0 ms; echo time, 90.0 ms; slice thickness, 4.0 mm; interslice gap, 2.0 mm; matrix, 300×189 ; field of view, $200 \text{ mm} \times 200 \text{ mm}$; flip angle, 90° ; and scan duration, 2 min 20 s. Thereafter, the patients underwent thin-sliced coronal and sagittal T2-weighted imaging covering the whole course of the ON in the cranial and orbital cavities. The following parameters were used for each sequence: repetition time, 3500.0 ms; echo

time, 90.0 ms; slice thickness, 2.0 mm; interslice gap, 0 mm; matrix, 300×189 ; field of view, $200 \text{ mm} \times 200 \text{ mm}$; flip angle, 90° ; and scan duration, 2 min 40 s. All examinations were performed using a 3.0-T MRI scanner (Achieva R2.6; Philips Medical Systems, Best, The Netherlands). The obtained imaging data were transferred to a workstation (Virtual Place Lexus64, 64 edition, AZE, Tokyo, Japan) and analyzed independently by two of the authors (S.T. and H.I.).

The present study was conducted in accordance with our institution's guidelines for human research. Written informed consent was obtained from all participants.

Observations of the intraorbital ON and relevant structures were performed by one of the authors (S.T.) through three injected cadaver heads at the Department of Neurological Surgery, University of Florida, Gainesville, FL, USA.

Results

Cadaver dissection

In the cadaver specimens, the optic sheath, intraorbital ON and surrounding subarachnoid spaces, and CRA coursing in the central part of the nerve were clearly identified in all sides of the three specimens, at both the level of the orbital apex and tip of the ON. In contrast, differences in appearance between the central and peripheral parts of the ON were not observed in any side. On coronal sections, the perivascular spaces of the CRA were ill-defined and not identified in any of the six ONs (Fig. 1).

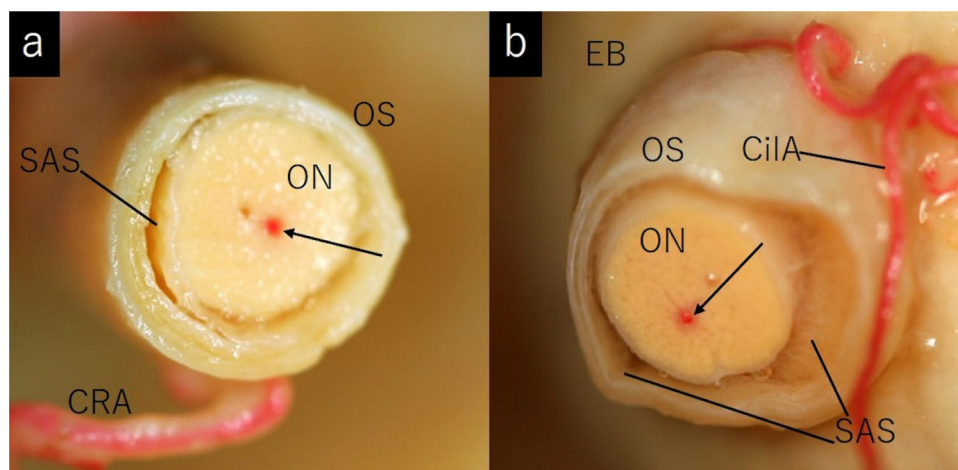


Fig. 1 **a, b** Coronal sections of a dissected right optic nerve at the level of the orbital apex, viewed from the front (**a**), and tip of the nerve, viewed from the rear (**b**), showing the optic sheath, intraorbital optic nerve and surrounding subarachnoid spaces, and central retinal artery coursing in the central part of the nerve. There is no difference

in appearance between the central and peripheral parts of the ON. The perivascular spaces of the central retinal artery are ill-defined. *CiA* ciliary artery, *CRA* central retinal artery, *EB* eyeball, *ON* optic nerve, *OS* optic sheath, *SAS* subarachnoid space, *arrow* central retinal artery

MRI

On axial T2-weighted MRI performed in the initial examination, the central part of some intraorbital ONs was delineated as a well-demarcated linear hyperintense area (Fig. 2). The finding was identified in 17 of 89 patients (19%), 9 on the right side and 11 on the left side. On the thin-sliced serial coronal images, hyperintense areas were identified on both sides in 81 patients (91%). They were delineated as continuous hyperintense areas in the ONs with an inconsistent appearance even in the same nerve, from the orbital apex to

its tip. In 11 patients (12.4%), the areas were divided into upper and lower parts by a horizontal septum, 9 on the right and 10 on the left. Other patients had hyperintense areas in the ONs with variable morphologies, lacking a septum (Fig. 3). These areas involved the central part of the ON and showed highly interindividual variability (Fig. 4). Furthermore, on the thin-sliced sagittal images, hyperintense areas were identified in 41 patients (46%), 30 on the right and 28 on the left, in variable parts of the intraorbital ONs (Fig. 5).

The identification rates of the hyperintense areas are summarized in Table 1.

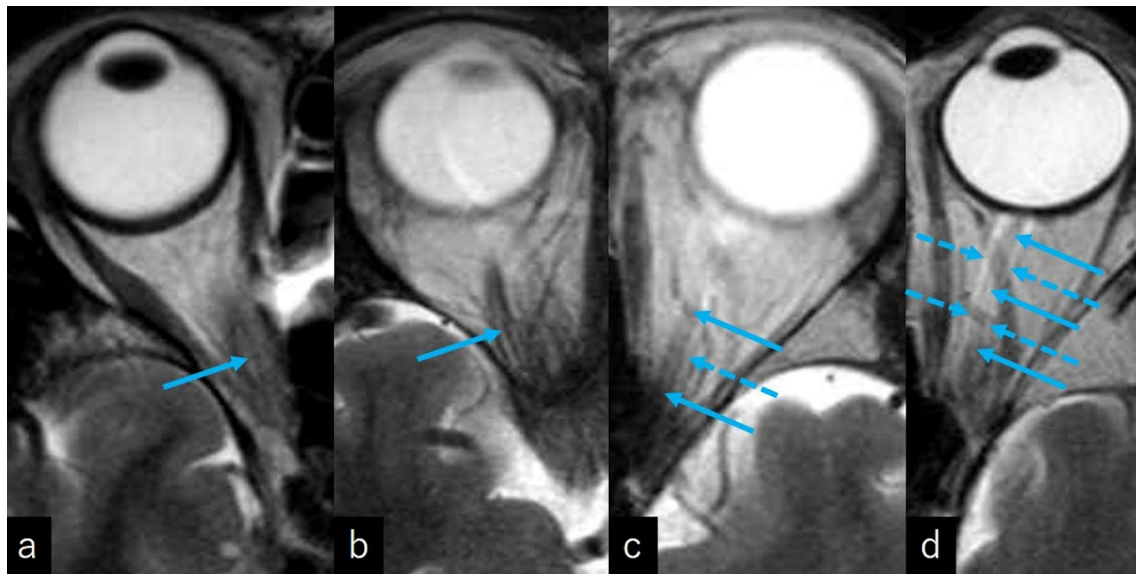
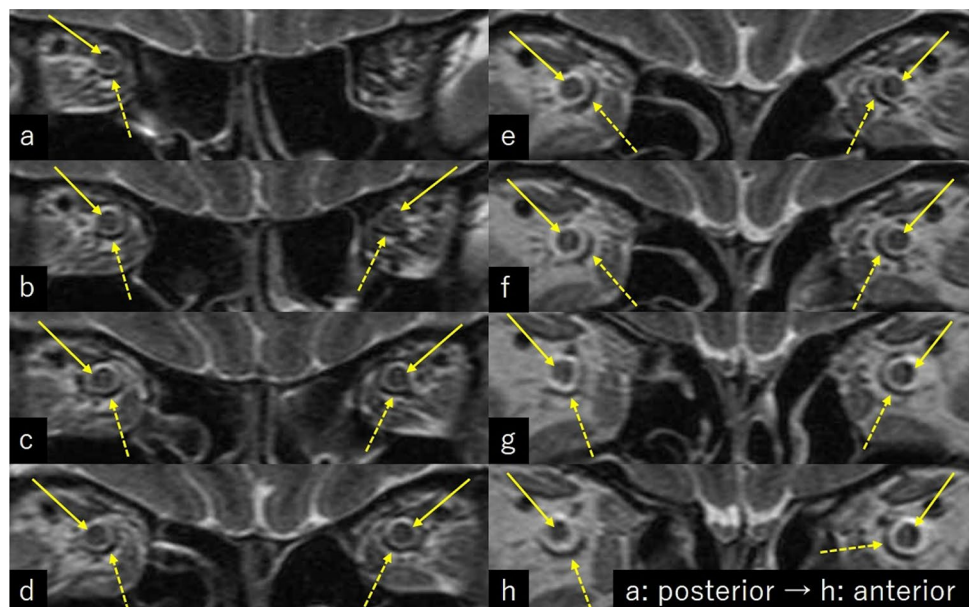


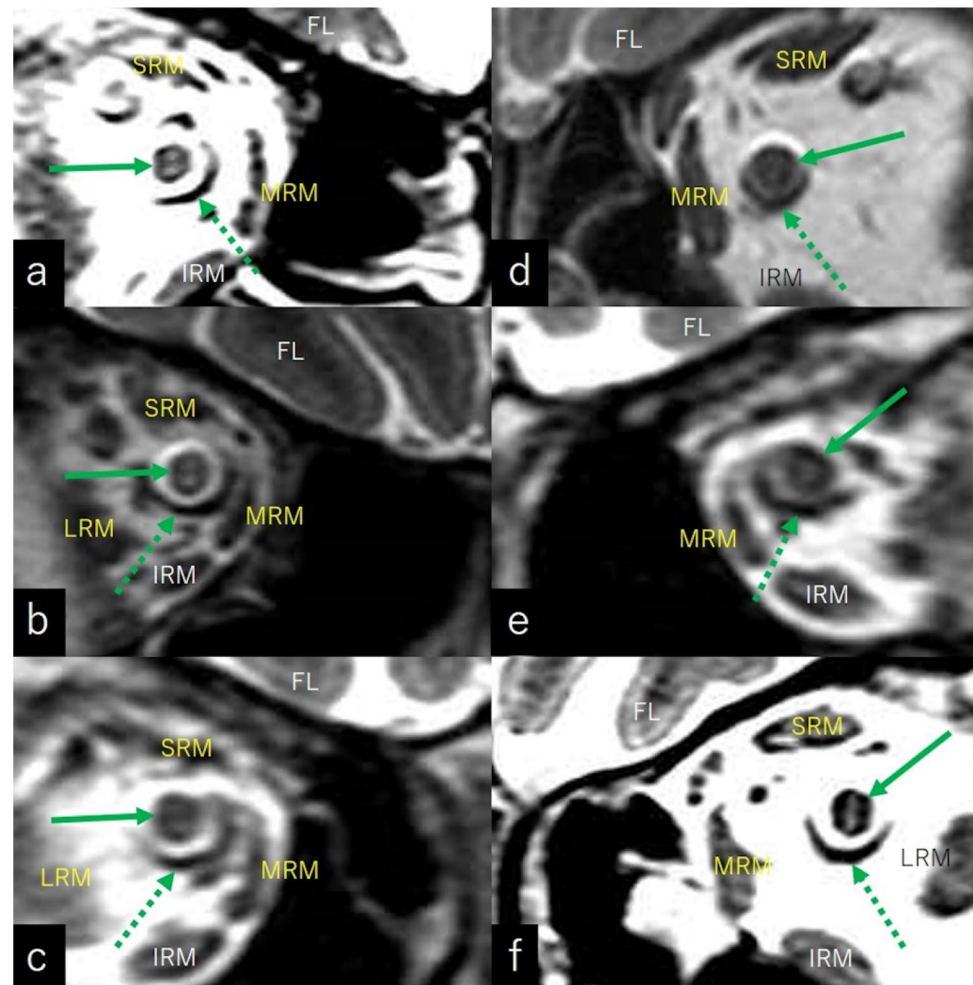
Fig. 2 a–d Axial T2-weighted magnetic resonance images of different patients in the initial examination, showing a well-demarcated, linear hyperintense area lying in the optic nerve (arrows). Dotted arrows: subarachnoid space. a, b right orbit; c, d left orbit

Fig. 3 a–h Serial coronal T2-weighted magnetic resonance images of a patient showing continuous but inconsistent hyperintense areas in the intraorbital optic nerve that distribute from the orbital apex to the posterior pole of the eyeball. Note that, in some images, the areas are divided into upper and lower parts by a horizontal septum, while others show variable morphologies, lacking a septum. Arrow: optic nerve; dotted arrow: optic sheath



a: posterior → h: anterior

Fig. 4 a–f Coronal T2-weighted magnetic resonance images of different patients showing hyperintense areas variably distributing in the intraorbital optic nerves. In a–c, the optic nerve is variably divided into upper and lower parts by a horizontal septum, while such septum is not found in d–f FL frontal lobe, IRM inferior rectus muscle, LRM lateral rectus muscle, MRM medial rectus muscle, SRM superior rectus muscle a–c right orbit; d–f left orbit; arrow optic nerve; dotted arrow: optic sheath



Discussion

In the present study, hyperintense areas in the intraorbital ONs were detected in > 90% of patients who underwent thin-sliced coronal T2-weighted imaging. These areas involved the central part of the ON. In contrast, these areas and those involving the perivascular spaces of the CRA were ill-defined in cadaver specimens. Studies have suggested that the perivascular spaces of the CRA may be major CSF inflow routes into the ON [8, 14, 17, 26]. Furthermore, evidence has shown that a glymphatic system exists in the ON [8, 10, 22]. Therefore, we assumed that the hyperintense areas identified in the present study may involve a glymphatic pathway with the perivascular spaces of the CRA. However, it should be noted that MRI does not allow direct visualization of the various glymphatic transport components, and that our observations do not prove the existence of a glymphatic system in the human ON. The areas were thought to be distinct regions in the normal ON, not representing some pathological findings. Given that the appearance of the areas showed

intraindividual variability, their function as glymphatic pathways may be diverse in different parts of the ON. In contrast, the anatomical and functional implications of the septum and divided hyperintense areas that were identified on the coronal images are elusive. As these fine internal structures may be difficult to identify, probably due to collapse on surgical and cadaver specimens, in vivo investigations seem to be advantageous. From the perspective of the imaging plane, the coronal sections seemed to be the most sensitive for detecting hyperintense areas in the ONs.

Previous studies have reported that intracranial pressure (ICP) is lower in patients with glaucoma compared with controls [2, 15, 16]. This gave rise to the idea that a lower ICP could cause glaucomatous ON damage, and that elevated ICP could provide a protective effort for the ON. Recently, Wostyn [24] hypothesized that the lower ICP reported in normal-tension glaucoma patients could lead to impaired CSF entry into perivascular spaces of the ON, given that the pressure generated through a constant production of CSF by the choroid plexus, among other

Fig. 5 a–f Sagittal T2-weighted magnetic resonance images of different patients showing hyperintense areas distributing in various parts of the optic nerve (arrows). a–c right orbit; d–f left orbit; dotted arrow: optic sheath

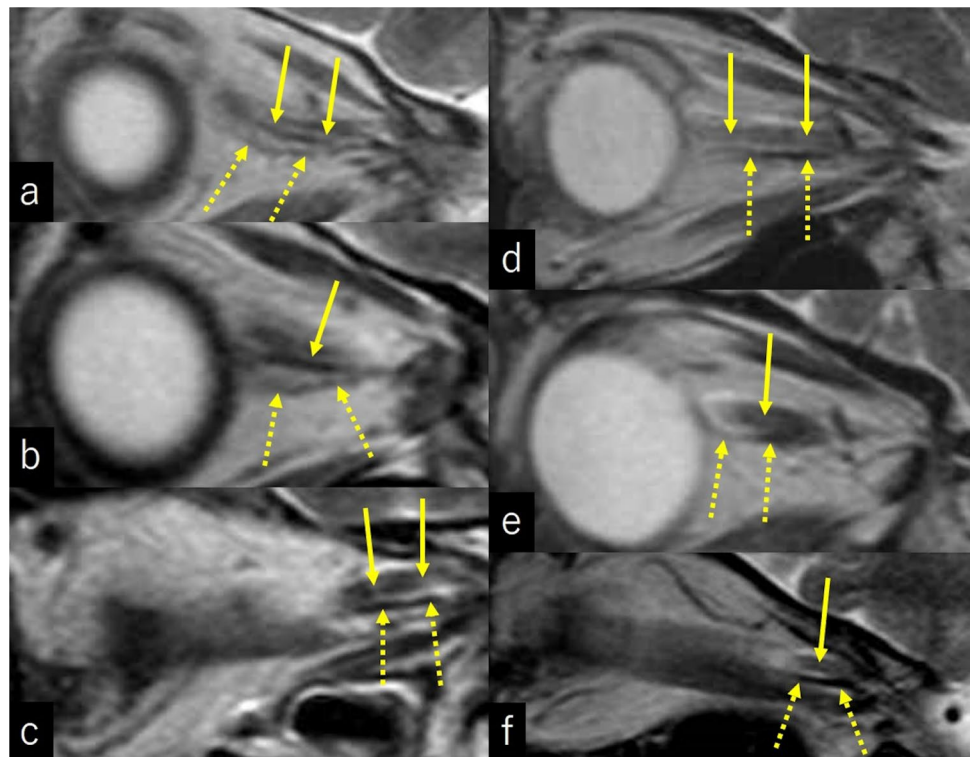


Table 1 Summary of identified hyperintense areas

| Sequence | Identified sides |
|----------|--------------------------------|
| Axial | 17 (19%) Right: 9, Left: 11 |
| Coronal | 81(91%) Right: 81, Left: 81 |
| Sagittal | 41(46%) Right: 30, Left: 28 |

factors, drives glymphatic fluid transport. The idea should be verified in the future study.

The present study has limitations. Our study was performed in a retrospective manner, with the participants not randomly assigned. The group of subjects was not age or sex matched. In addition, the hyperintense areas in the ONs were assessed only on T2-weighted images. Furthermore, the number of dissected specimens was small to conclude that the perivascular spaces of the CRA were difficult to identify on cadaver dissection. Detailed microscopic exploration of the perivascular spaces of the ON and CRA is also necessary in future investigations. Despite these limitations, we believe that the findings provided by our methodology suggest that the hyperintense areas identified in the intraorbital ONs may involve a glymphatic pathway.

Conclusion

Hyperintense areas in the intraorbital ON detected on T2-weighted imaging may involve a glymphatic pathway with perivascular spaces of the ON and CRA. These may be collapsed and difficult to identify in surgical and cadaver specimens.

Acknowledgements This study did not receive any grant funding.

Author contributions ST and HO developed the study project. ST performed cadaver dissection. HO performed examinations using magnetic resonance imaging. HI collected and managed the data. ST and HI analyzed the data. ST wrote the manuscript.

Compliance with ethical standards

Conflict of interest The authors have no conflicts of interest concerning the materials and methods used in this study or the findings presented in this manuscript.

References

- Baneke AJ, Aubry J, Viswanathan AC, Plant GT (2020) The role of intracranial pressure in glaucoma and therapeutic implications. *Eye (Lond)* 34:178–191
- Berdahl JP, Fautsch MP, Stinnett SS, Allingham RR (2008) Intracranial pressure in primary open angle glaucoma, normal tension glaucoma, and ocular hypertension: a case-control study. *Invest Ophthalmol Vis Sci* 49:5412–5418

3. Furlanetto RL, Teixeira SH, Gracitelli CRB, Lottenberg CL, Emori F, Michelan M, Amaro E Jr, Paranhos A Jr (2018) Structural and functional analyses of the optic nerve and lateral geniculate nucleus in glaucoma. *PLoS ONE* 13:e0194038
4. Garaci FG, Bolacchi F, Cerulli A, Melis M, Spanò A, Cedrone C, Floris R, Simonetti G, Nucci C (2009) Optic nerve and optic radiation neurodegeneration in patients with glaucoma: in vivo analysis with 3-T diffusion-tensor MR imaging. *Radiology* 252:496–501
5. Hablitz LM, Plá V, Gianetto M, Vinitsky H, Stæger FF, Metcalfe T, Nguyen R, Benrais A, Nedergaard M (2020) Circadian control of brain glymphatic and lymphatic fluid flow. *Nat Commun* 11:4411
6. Hao J, Pircher A, Miller NR, Hsieh J, Remonda L, Killer HE (2020) Cerebrospinal fluid and optic nerve sheath compartment syndrome: a common pathophysiological mechanism in five different cases? *Clin Exp Ophthalmol* 48:212–219
7. Iliff JJ, Wang M, Liao Y, Plogg BA, Peng W, Gundersen GA, Benveniste H, Vates GE, Deane R, Godman SA, Nagelhus EA, Nedergaard M (2012) A paravascular pathway facilitates CSF flow through the brain parenchyma and the clearance of interstitial solutes, including amyloid β . *Sci Transl Med* 4:147ra111
8. Jacobsen HH, Ringstad G, Jørstad ØK, Moe MC, Sandell T, Eide PK (2019) The human visual pathway communicates directly with the subarachnoid space. *Invest Ophthalmol Vis Sci* 60:2773–2780
9. Killer HE, Laeng HR, Flammer J, Groscurth P (2003) Architecture of arachnoid trabeculae, pillars, and septa in the subarachnoid space of the human optic nerve: anatomy and clinical considerations. *Br J Ophthalmol* 87:777–781
10. Mathieu E, Gupta N, Ahari A, Zhou X, Hanna J, Yücel YH (2017) Evidence for cerebrospinal fluid entry into the optic nerve via a glymphatic pathway. *Invest Ophthalmol Vis Sci* 58:4784–4791
11. Mathieu E, Gupta N, Paczka-Giorgi LA, Zhou X, Ahari A, Lani R, Hanna J, Yücel YH (2018) Reduced cerebrospinal fluid inflow to the optic nerve in glaucoma. *Invest Ophthalmol Vis Sci* 59:5876–5884
12. Mestre H, Mori Y, Nedergaard M (2020) The brain's glymphatic system: current controversies. *Trends Neurosci* 43:458–466
13. Mirra S, Marfany G, Garcia-Fernández J (2020) Under pressure: Cerebrospinal fluid contribution to the physiological homeostasis of the eye. *Semin Cell Dev Biol* 102:40–47
14. Papp A, Tóth J, Kerényi T, Jäckel M, Süveges I (2004) Silicone oil in the subarachnoidal space – a possible route to the brain? *Pathol Res Pract* 200:347–352
15. Price DA, Harris A, Siesky B, Mathew S (2020) The influence of translaminar pressure gradient and intracranial pressure in glaucoma: a review. *J Glaucoma* 29:141–146
16. Ren R, Jonas JB, Tian G, Zhen Y, Ma K, Li S, Wang H, Li B, Zhang X, Wang N (2010) Cerebrospinal fluid pressure in glaucoma: a prospective study. *Ophthalmology* 117:259–266
17. Sakamoto M, Nakamura K, Shibata M, Yokoyama K, Matsui M, Ikeda T (2010) Magnetic resonance imaging findings of Terson's syndrome suggesting a possible vitreous hemorrhage mechanism. *Jpn J Ophthalmol* 54:135–139
18. Sartoretti T, Stürmer J, Sartoretti E, Najafi A, Schwenk Á, Wyss M, Binkert C, Sartoretti-Schefer S (2019) Long segment 3D double inversion recovery (DIR) hypersignal on MRI in glaucomatous optic neuropathy. *BMC Ophthalmol* 19:258
19. Wostyn P, Van Dam D, Audenaert K, Killer HE, De Deyn PP, De Groot V (2015) A new glaucoma hypothesis: a role of glymphatic system dysfunction. *Fluids Barriers CNS* 12:16
20. Wostyn P, De Groot V, Van Dam D, Audenaert K, De Deyn PP, Killer HE (2016) The glymphatic system: a new player in ocular diseases? *Invest Ophthalmol Vis Sci* 57:5426–5427
21. Wostyn P, Killer HE, De Deyn PP (2017) Glymphatic stasis at the site of the lamina cribrosa as a potential mechanism underlying open-angle glaucoma. *Clin Exp Ophthalmol* 45:539–547
22. Wostyn P, De Groot V, Van Dam D, Audenaert K, Killer HE, De Deyn PP (2017) The glymphatic hypothesis of glaucoma: a unifying concept incorporating vascular, biomechanical, and biochemical aspects of the disease. *Biomed Res Int* 2017:5123148
23. Wostyn P, De Groot V, Van Dam D, Audenaert K, De Deyn PP, Killer HE (2018) The first histologic evidence of a paravascular pathway within the optic nerve. *Invest Ophthalmol Vis Sci* 59:1717
24. Wostyn P (2019) Glaucoma as a dangerous interplay between ocular fluid and cerebrospinal fluid. *Med Hypotheses* 127:97–99
25. Wostyn P, Mader TH, Gibson CR, Killer HE (2020) The perivascular space of the central retinal artery as a potential major cerebrospinal fluid inflow route: Implications for optic disc edema in astronauts. *Eye (Lond)* 34:779–780
26. Yiannakas MC, Toosy AT, Raftopoulos RE, Kapoor R, Miller DH, Wheeler-Kingshott CA (2013) MRI acquisition and analysis protocol for in vivo intraorbital optic nerve segmentation at 3T. *Invest Ophthalmol Vis Sci* 54:4235–4240
27. Zhang YQ, Li J, Xu L, Zhang L, Wang ZC, Yang H, Chen CX, Wu XS, Jonas JB (2012) Anterior visual pathway assessment by magnetic resonance imaging in normal-pressure glaucoma. *Acta Ophthalmol* 90:e295–e302

Publisher's Note Springer Nature remains neutral with regard to jurisdictional claims in published maps and institutional affiliations.